

# Optical design of a Sagnac-Speedmeter

## Proof of Principle Experiment



Stewart Rigby (supervisor S.Hild)  
0905393r@students.gla.ac.uk



### Introduction

Michelson interferometers have traditionally been utilised as large scale gravitational wave detectors, but after years of development we are close to the quantum limit of sensitivity (SQL). A Michelson continuously measures mirror position which is limited by quantum mechanics.

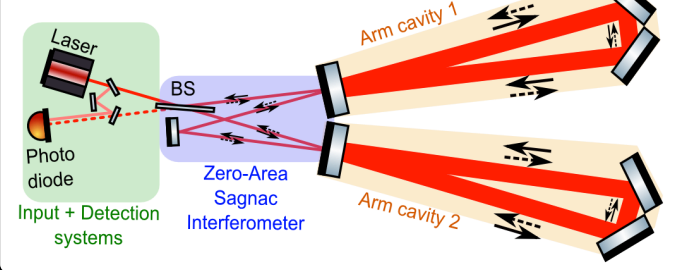
$$[\hat{x}(t), \hat{x}(t')] \neq 0$$

A new approach to beat the standard quantum limit is to use an interferometer designed around the speedmeter principle. It has been shown that a speedmeter is not bound by the Heisenberg uncertainty principle as a Speedmeter measures the momentum of a free test mass.

$$[\hat{p}(t), \hat{p}(t')] = 0$$

A zero area Sagnac interferometer has been shown to be a speedmeter<sup>[1]</sup> and is also suitable to be used as a large scale interferometer as it will occupy the same L shaped footprint as current Michelson's. Here we examine the differences between the Michelson and Sagnac interferometers and then examine the optical design of a new zero area Sagnac illustrated below.

### Optical Layout of proposed Sagnac



### Cavity optical design

Design considerations: Three mirror ring cavity, arm lengths allow assembly within the designated area. Large beam radii on mirrors reduce noise, restricted by mirror radius. Symmetric layout illustrated below.

- \* Z = Distance from waist.
- \* L = Cavity length.
- \* ω<sub>0</sub> = Beam waist, Radius at Z=0.
- \* Z<sub>R</sub> = Rayleigh length.
- \* ω<sub>(z)</sub> = Radius distance Z from waist.

Design Process: Resonance requires radius of curvature (RoC) of the mirror to match the RoC of the wavefront. Using the relations above, the waist radius is calculated. Two waists sizes possible for 1mm spot size at mirror, very large or very small. Small waist for A2 arm of order 10<sup>-7</sup>m is problematic, large waist of 10<sup>-3</sup>m chosen. Complex beam parameter and ABCD matrices used for full cavity calculation.

Resonance condition met when q<sub>in</sub>=q<sub>out</sub> after one round trip.

$$\frac{1}{q} = \frac{1}{R(z)} - i \frac{\pi \omega^2(z)}{\lambda} \begin{bmatrix} A & B \\ C & D \end{bmatrix} \begin{bmatrix} 1 & 0 \\ -2/R & 1 \end{bmatrix} \begin{bmatrix} 1 & L \\ 0 & 1 \end{bmatrix}$$

Complex beam parameter    Matrices    Mirror    Space

$$q_{out} = \frac{Aq_{in} + B}{Cq_{in} + D} \quad -1 < \frac{1}{2}(A+D) < 1$$

Beam parameter transform    Cavity stability

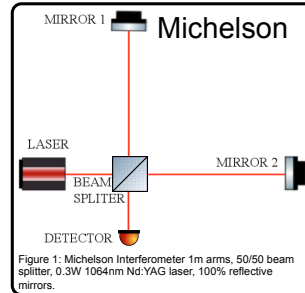


Figure 1: Michelson Interferometer 1m arms, 50/50 beam splitter, 0.3W 1064nm Nd:YAG laser, 100% reflective mirrors.

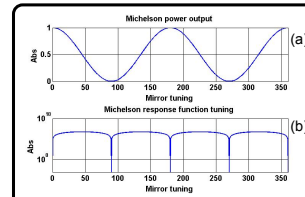


Figure 3a: Mirror 2 tuned over 1 wavelength. Power dependent on difference in arm length. Figure 3b: Differential signal applied to arms. Zero response corresponds to equal arms lengths. Small difference in arm length required to offset from dark fringe.

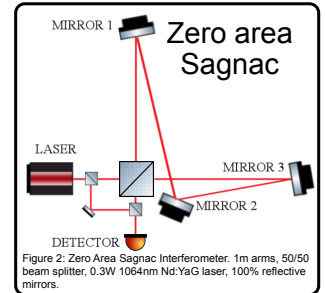


Figure 2: Zero Area Sagnac Interferometer. 1m arms, 50/50 beam splitter, 0.3W 1064nm Nd:YAG laser, 100% reflective mirrors.

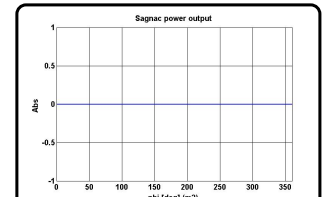


Figure 4: Mirror 3 is tuned over 1 wavelength. Power is independent of difference in arm length. Unlike the Michelson the Sagnac always operates on a dark fringe, avoiding the need for small difference in arm length.

### Michelson Interferometer Response

$$E_{in} = E_0 \cos(\omega_s t) \quad E_{out} = E_0 \cos(\omega_s t + \phi)$$

$$h_x = h_0 \cos(\omega_s t')$$

$$\phi = \frac{2L}{c} \omega_0 + \frac{\omega_0}{2} \int_{-L/c}^{L/c} h_x(t') dt'$$

$$\phi = \frac{2L}{c} \omega_0 + \frac{h_0 \omega_0}{\omega_s} \sin\left(\omega_s \frac{L}{c}\right) \cos\left(\omega_s \left(t - \frac{L}{c}\right)\right)$$

EM wave E<sub>in</sub> enters an arm of the Michelson, length L, exits at the beam splitter as E<sub>out</sub> with phase φ. If a gravitational wave, strain h<sub>x</sub>, is encountered there is an additional phase shift. The GW is integrated into φ back along the path taken, from t to t-L/c. (Figure 5b) The plot of the geometry term (a), agrees with the Finesse model (Figure 5a).

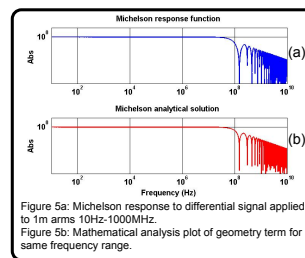


Figure 5a: Michelson response to differential signal applied to 1m arms 10Hz-1000MHz. Figure 5b: Mathematical analysis plot of geometry term for same frequency range.

### Sagnac interferometer response

$$\phi_1 = \frac{4L}{c} \omega_0 + \frac{\omega_0}{2} \left[ \int_{-L/c}^{L/c} h_x(t') dt' - \int_{-L/c}^{L/c} h_x(t') dt' \right]$$

$$\phi_2 = \frac{4L}{c} \omega_0 + \frac{\omega_0}{2} \left[ - \int_{-L/c}^{L/c} h_x(t') dt' + \int_{-L/c}^{L/c} h_x(t') dt' \right]$$

$$|\Delta\phi| = \frac{4h_0 \omega_0}{\omega_s} \sin\left(\omega_s \frac{L}{c}\right) \cos\left(\omega_s \left(t - \frac{L}{c}\right)\right)$$

The Sagnac is analysed in the same manner as the Michelson. Both paths are integrated along both arms. The phase difference is calculated. The geometry term (a) is plotted in (Figure 6b), agrees with the Finesse model (Figure 6a).

The peak response for the Michelson is independent of signal at low frequencies. (Figure 5)

The peak response for the Sagnac scales with signal at low frequencies. (Figure 6)

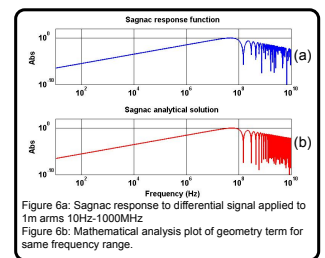


Figure 6a: Sagnac response to differential signal applied to 1m arms 10Hz-1000MHz. Figure 6b: Mathematical analysis plot of geometry term for same frequency range.

